

Spin Conversion versus Antiferromagnetic Interaction in Iron(II) Trinuclear Species. Crystal Structures and Magnetic Properties of $[\text{Fe}_3(p\text{-MeOptrz})_8(\text{H}_2\text{O})_4](\text{BF}_4)_6$ and $[\text{Fe}_3(p\text{-MeOptrz})_6(\text{H}_2\text{O})_6](\text{tos})_6$ [$p\text{-MeOptrz} = 4\text{-(}p\text{-Methoxyphenyl)-1,2,4-triazole}$, $\text{tos} = \text{Tosylate}$]

Martina Thomann,[†] Olivier Kahn,^{*,†} Jean Guilhem,[‡] and François Varret[§]

Laboratoire de Chimie Inorganique, URA No. 420, Université de Paris Sud, 91405 Orsay, France, Institut de Chimie des Substances Naturelles, UPR No. 2301, 91198 Gif-sur-Yvette, France, and Département de Recherches Physiques, URA No. 71, Université Pierre et Marie Curie, 75232 Paris, France

Received May 18, 1994[®]

By reaction of iron(II) salts with 4-(*p*-methoxyphenyl)-1,2,4-triazole, hereafter abbreviated as *p*-MeOptrz, two compounds have been synthesized, namely $[\text{Fe}_3(p\text{-MeOptrz})_8(\text{H}_2\text{O})_4](\text{BF}_4)_6$ (**1**) and $[\text{Fe}_3(p\text{-MeOptrz})_6(\text{H}_2\text{O})_6](\text{tos})_6$ (**2a**). The crystal structures have been solved at room temperature. Both compounds crystallize in the triclinic system, space group $P\bar{1}$. The lattice parameters are as follows: for **1**·2H₂O, $a = 15.107(7)$ Å, $b = 14.678(7)$ Å, $c = 12.392(6)$ Å, $\alpha = 112.14(6)^\circ$, $\beta = 95.85(5)^\circ$, $\gamma = 104.40(6)^\circ$, $Z = 1$; for **2a**·2CH₃OH·8H₂O, $a = 12.983(5)$ Å, $b = 16.324(7)$ Å, $c = 17.362(8)$ Å, $\alpha = 105.28(3)^\circ$, $\beta = 109.34(4)^\circ$, $\gamma = 106.94(4)^\circ$, $Z = 1$. Both structures consist of linear trinuclear cations with a +6 charge, and noncoordinated anions and solvent molecules. The central iron atom lies on an inversion center and is triply bridged to each of the external iron atoms by the *p*-MeOptrz ligands through the nitrogen atoms in the 1,2-positions. Each external iron atom completes its octahedral surroundings with one *p*-MeOptrz ligand and two water molecules in **1** and with three water molecules in **2a**. The average value of the dihedral angle between triazole and phenyl rings of the bridging ligands is equal to 71.4° in **1** and 33.2° in **2a**. Heating **2a** at 100°C affords a compound **2b** of formula $[\text{Fe}_3(p\text{-MeOptrz})_6(\text{H}_2\text{O})_3](\text{tos})_6$. The magnetic properties of **1**, **2a**·4H₂O, and **2b** have been investigated. For **1**, the three iron(II) ions are high-spin in the whole temperature range. The temperature dependence of the molar magnetic susceptibility has been quantitatively interpreted by full diagonalization of the spin Hamiltonian, taking into account the isotropic interaction between nearest neighbor spin carriers, and the local anisotropies. The interaction parameter between central and external iron(II) ions has been found at $J = -5.7\text{ cm}^{-1}$ ($\mathbf{H} = -J\mathbf{S}_A \cdot \mathbf{S}_B$). For **2a**·4H₂O and **2b** the central iron(II) ion undergoes a gradual spin conversion centered at $T_{1/2} = 245$ and 330 K , respectively. This spin conversion has also been studied by Mössbauer spectroscopy. The switching between high-spin and spin-conversion situations when passing from **1** to **2a** has been attributed to the variation of the dihedral angle within the *p*-MeOptrz bridging ligands, caused in this instance by the nature of the anion.

Introduction

In some transition metal compounds, in particular those containing $3d^4$ – $3d^7$ metal ions in octahedral surroundings, a transition between a low-spin (LS) and a high-spin (HS) state may occur. This spin transition (ST) may be induced by a variation of temperature or pressure or by an irradiation with light. LS \leftrightarrow HS conversions were observed for the first time more than 50 years ago.¹ However, the interest raised by this phenomenon has known a new impetus in the last 2 decades.^{2–17}

One of our main interests in this area concerns the bistability exhibited by some ST compounds. Bistability is defined here as the possibility for a compound to show two stable or metastable states in a given external perturbation range. This bistability confers a memory effect on the system.^{18,19}

Three years ago, we initiated a new research project, the goal of which was to design devices for display or recording that incorporated ST compounds as active elements.^{20–22} Along this line we explored the iron(II)–1,2,4-*H*-triazole system and characterized several compounds exhibiting ST above or around

[†] Université de Paris Sud.

[‡] Institut de Chimie des Substances Naturelles.

[§] Université Pierre et Marie Curie.

[®] Abstract published in *Advance ACS Abstracts*, November 15, 1994.

- (1) Cambi, L.; Szegő, L. *Ber. Dtsch. Chem. Ges.* **1931**, *64*, 259. *Ibid.* **1933**, *66*, 656.
- (2) Goodwin, H. A. *Coord. Chem. Rev.* **1976**, *18*, 293.
- (3) Gütllich, P. *Struct. Bonding (Berlin)* **1981**, *44*, 83.
- (4) König, E.; Ritter, G.; Kulshreshtha, S. K. *Chem. Rev.* **1985**, *85*, 219.
- (5) Beattie, J. K. *Adv. Inorg. Chem.* **1988**, *32*, 1.
- (6) Gütllich, P.; Hauser, A. *Coord. Chem. Rev.* **1990**, *97*, 1.
- (7) König, E. *Prog. Inorg. Chem.* **1987**, *35*, 527.
- (8) König, E. *Struct. Bonding (Berlin)* **1991**, *76*, 51.
- (9) Bolvin, H.; Kahn, O. *Chem. Phys.*, submitted.
- (10) Descourtins, S.; Gütllich, P.; Köhler, C. P.; Hauser, A.; Spiering, H.; *Chem. Phys. Lett.* **1985**, *105*, 1.
- (11) Descourtins, S.; Gütllich, P.; Hasselbach, K. M.; Spiering, H.; Hauser, A. *Inorg. Chem.* **1985**, *24*, 2174.
- (12) Poganiuch, P.; Descourtins, S.; Gütllich, P. *J. Am. Chem. Soc.* **1990**, *112*, 3270.
- (13) Köppen, H.; Müller, E. W.; Köhler, C. P.; Spiering, H.; Meissner, E.; Gütllich, P. *Chem. Phys. Lett.* **1982**, *91*, 248.
- (14) Petrouleas, V.; Tuchagues, J. P. *Chem. Phys. Lett.* **1987**, *137*, 21.
- (15) Real, J. A.; Bolvin, H.; Bousseksou, A.; Dworkin, A.; Kahn, O.; Varret, F.; Zarembowitch, J. *J. Am. Chem. Soc.* **1992**, *114*, 4650.
- (16) Zarembowitch, J.; Roux, C.; Boillot, M. L.; Claude, R.; Itié, J. P.; Polian, A.; Bolte, M. *Mol. Cryst. Liq. Cryst.* **1993**, *234*, 247.
- (17) Adams, D. M.; Dei, A.; Rheingold, A. L.; Hendrickson, D. N. *J. Am. Chem. Soc.* **1993**, *115*, 8221.
- (18) Kahn, O.; Launay, J. P. *Chemtronics* **1988**, *3*, 140.
- (19) Zarembowitch, J.; Kahn, O. *New J. Chem.* **1991**, *15*, 181.
- (20) Kahn, O.; Kröber, J.; Jay, C. *Adv. Mater.* **1992**, *4*, 718.
- (21) Jay, C.; Grolière, F.; Kahn, O.; Kröber, J. *Mol. Cryst. Liq. Cryst.* **1993**, *234*, 255.
- (22) Kröber, J.; Codjovi, E.; Kahn, O.; Grolière, F.; Jay, C. *J. Am. Chem. Soc.* **1993**, *115*, 9810.

Table 1. Crystallographic Data for $[\text{Fe}_3(p\text{-MeOtrz})_8(\text{H}_2\text{O})_4](\text{BF}_4)_2 \cdot 2\text{H}_2\text{O}$ ($1 \cdot 2\text{H}_2\text{O}$)

chem formula: $\text{C}_{72}\text{H}_{84}\text{N}_{24}\text{O}_{14}\text{B}_6\text{F}_{24}\text{Fe}_3$	fw = 2198.03
$a = 15.107(7) \text{ \AA}$	space group: $P\bar{1}$
$b = 14.678(7) \text{ \AA}$	$T = 294 \text{ K}$
$c = 12.392(6) \text{ \AA}$	$\lambda = 0.71073 \text{ \AA}$
$\alpha = 112.14(6)^\circ$	$\rho_{\text{calc}} = 1.517 \text{ g cm}^{-3}$
$\beta = 95.85(5)^\circ$	$\mu = 0.56 \text{ mm}^{-1}$
$\gamma = 104.40(6)^\circ$	$R^a = 0.084$
$V = 2406(2) \text{ \AA}^3$	$R_w^b = 0.080$
$Z = 1$	

$^a R = \sum[|F_o| - |F_c|]/\sum|F_o|$. $^b R_w = [\sum[w(|F_o| - |F_c|)^2]]^{1/2}$ with $w = 4F_o^2/[\sigma^2(F_o^2) + (0.0012F_o^2)^2]$.

Table 2. Crystallographic Data for $[\text{Fe}_3(p\text{-MeOtrz})_6(\text{H}_2\text{O})_6](\text{tos})_6 \cdot 2\text{CH}_3\text{OH} \cdot 8\text{H}_2\text{O}$ ($2a \cdot 2\text{CH}_3\text{OH} \cdot 8\text{H}_2\text{O}$)

chem formula: $\text{C}_{98}\text{H}_{132}\text{H}_{18}\text{O}_{34}\text{S}_6\text{Fe}_3$	fw = 2413.19
$a = 12.983(5) \text{ \AA}$	space group: $P\bar{1}$
$b = 16.324(7) \text{ \AA}$	$T = 294 \text{ K}$
$c = 17.362(8) \text{ \AA}$	$\lambda = 0.71073 \text{ \AA}$
$\alpha = 105.28(3)^\circ$	$\rho_{\text{calc}} = 1.316 \text{ g cm}^{-3}$
$\beta = 109.34(4)^\circ$	$\mu = 0.38 \text{ mm}^{-1}$
$\gamma = 106.94(4)^\circ$	$R^a = 0.050$
$V = 3046(4) \text{ \AA}^3$	$R_w^b = 0.054$
$Z = 1$	

$^a R = \sum[|F_o| - |F_c|]/\sum|F_o|$. $^b R_w = [\sum[w(|F_o| - |F_c|)^2]]^{1/2}$ with $w = 4F_o^2/[\sigma^2(F_o^2) + (0.0012F_o^2)^2]$.

room temperature with thermal hysteresis widths as large as ca. 50 K. Recently, Goodwin reported on the same family of compounds.²³ These compounds have a polymeric structure, and obtaining single crystals suitable for X-ray diffraction seems to be very problematic. In order to get more structural information, and if possible to tune the ST characteristics, we also investigated some iron(II)–4-substituted-1,2,4-triazole systems. A series of isomorphous trinuclear compounds with the composition $[\text{M}_3(\text{Etrtz})_6(\text{H}_2\text{O})_6](\text{CF}_3\text{SO}_3)_6$ in which M is a divalent metal ion has been described by Reedijk and co-workers.²⁴ For M = Fe(II) the central iron(II) ion undergoes a gradual spin conversion while the two external metal ions are high-spin in the whole temperature range. In this paper we report on the results obtained with the ligand 4-(*p*-methoxyphenyl)-1,2,4-triazole, hereafter abbreviated as *p*-MeOtrz. Two trinuclear compounds the formulas of which are $[\text{Fe}_3(p\text{-MeOtrz})_8(\text{H}_2\text{O})_4](\text{BF}_4)_6$ (**1**) and $[\text{Fe}_3(p\text{-MeOtrz})_6(\text{H}_2\text{O})_6](\text{tos})_6$ (**2a**) with *tos* = tosylate were synthesized. We will describe the crystal structures of **1**·2H₂O and **2**·2CH₃OH·8H₂O and the magnetic properties of **1** and **2a**·4H₂O. Heating **2a**·4H₂O at 100 °C affords the compound **2b** of formula $[\text{Fe}_3(p\text{-MeOtrz})_6(\text{H}_2\text{O})_3](\text{tos})_6$ that we also investigated.

Experimental Section

Syntheses. The ligand 4-(*p*-methoxyphenyl)-1,2,4-triazole (*p*-MeOtrz) was obtained according to a modified literature procedure.²⁵ A mixture of 16.2 g (132 mmol) of *syn*-diformylhydrazine and 11.6 g (132 mmol) of *p*-methoxyaniline were heated for 1 h at 190 °C. After cooling to room temperature the oily product was purified by chromatography over a 32 cm long basic alumina column, using a 10/30 methanol/ether mixture as eluant; *p*-MeOtrz was found in the second fraction and was identified by IR ($\nu = 3143$ and 3125 cm^{-1}). A 8.73 g (42 mmol) portion of the ligand was obtained (yield: 32%). ¹H (CDCl₃, TMS): 8.42 (2H, triazole), 7.32 (2H, d, 8.5 Hz), 7.04 (2H, d, 8.6 Hz), 3.88 (3H, methyl). ¹³C (CDCl₃, TMS): 159.6 (*p*-C), 141.6 (triazole), 126.4 (*ipso*-C), 123.6 (*o*-C), 114.9 (*m*-C), 55.4 (methyl). The trinuclear species $[\text{Fe}_3(p\text{-MeOtrz})_8(\text{H}_2\text{O})_4](\text{BF}_4)_6$ (**1**) was obtained as

Table 3. Atomic Coordinates ($\times 10^4$) and Equivalent Isotropic Thermal Factors ($\times 10^3$) for the Non-Hydrogen Atoms of $[\text{Fe}_3(p\text{-MeOtrz})_8(\text{H}_2\text{O})_4](\text{BF}_4)_2 \cdot 2\text{H}_2\text{O}$ ($1 \cdot 2\text{H}_2\text{O}$)^a

	X	Y	Z	U ^b
Fe1	5000	5000	5000	43(4)
Fe2	4194(1)	3009(2)	6323(2)	47(3)
N1a	4169(7)	5184(9)	6420(9)	41(16)
N2a	3922(7)	4436(9)	6864(9)	47(17)
C3a	3379(10)	4796(12)	7594(12)	46(22)
N4a	3281(8)	5678(10)	7631(10)	53(19)
C5a	3794(9)	5852(11)	6856(13)	48(22)
C6a	2642(7)	6171(9)	8200(10)	62(24)
C7a	2903(7)	6827(9)	9415(10)	97(32)
C8a	2276(7)	7292(9)	9979(10)	108(35)
C9a	1389(7)	7100(9)	9330(10)	89(31)
C10a	1128(7)	6444(9)	8115(10)	70(26)
C10a	1754(7)	5979(9)	7551(10)	71(27)
O12a	801(9)	7557(11)	9925(11)	126(25)
C13a	-66(15)	7455(19)	9288(21)	173(49)
N1b	4080(7)	3452(9)	4005(9)	44(16)
N2b	3768(8)	2714(10)	4480(10)	54(19)
C3b	3279(10)	1854(12)	3586(14)	49(22)
N4b	3202(8)	1965(10)	2563(10)	54(19)
C5b	3699(10)	2946(12)	2862(13)	49(22)
C6b	2710(8)	1208(8)	1394(7)	53(23)
C7b	1787(8)	1113(8)	961(7)	88(30)
C8b	1317(8)	383(8)	-189(7)	83(30)
C9b	1771(8)	-252(8)	-905(7)	60(25)
C10b	2694(8)	-158(8)	-473(7)	88(31)
C11b	3163(8)	572(8)	677(7)	89(31)
O12b	1284(8)	-886(9)	-2016(9)	78(18)
C13b	1675(13)	-1534(14)	-2806(15)	84(29)
N1c	4068(7)	5523(9)	4124(10)	46(17)
N2c	4368(7)	6279(10)	3685(9)	51(18)
C3c	3644(11)	6465(12)	3287(13)	68(25)
N4c	2859(8)	5891(9)	3427(10)	46(17)
C5c	3155(10)	5335(11)	3960(13)	53(22)
C6c	1958(5)	5929(8)	3113(9)	46(21)
C7c	1371(5)	5997(8)	3921(9)	66(25)
C8c	483(5)	6070(8)	3629(9)	76(27)
C9c	181(5)	6075(8)	2530(9)	52(23)
C10c	768(5)	6008(8)	1723(9)	63(24)
C11c	1565(5)	5935(8)	2014(9)	65(25)
O12c	-670(7)	6180(9)	2334(10)	85(18)
C13c	-1000(12)	6209(17)	1251(17)	122(38)
N1d	2884(10)	1345(12)	6781(15)	116(29)
N2d	2836(9)	2096(10)	6386(11)	70(21)
C3d	1979(11)	2139(12)	6237(14)	70(25)
N4d	1429(8)	1406(10)	6506(10)	58(19)
C5d	1988(13)	960(14)	6863(19)	113(36)
C6d	467(6)	1142(9)	6472(10)	53(22)
C7d	-102(6)	1482(9)	5853(10)	89(30)
C8d	-1050(6)	1283(9)	5881(10)	91(30)
C9d	-1429(6)	743(9)	6528(10)	73(27)
C10d	-860(6)	402(9)	7148(10)	142(42)
C11d	88(6)	602(9)	7120(10)	121(36)
O12d	-2342(8)	521(10)	6615(12)	113(23)
C13d	-2911(12)	922(16)	6119(21)	136(42)
W1	4707(7)	3365(8)	8173(8)	74(16)
W2	4555(7)	1598(8)	5836(9)	78(17)
W3***	4646(25)	1757(27)	9098(32)	177(14)
W4***	5167(25)	1359(28)	7877(33)	184(14)
B1	3408(5)	4136(6)	451(6)	92(43)
F11	3523(5)	5041(6)	454(6)	188(29)
F21	2806(5)	3978(6)	1087(6)	174(26)
F31	3102(5)	3433(6)	-635(6)	110(18)
F41	4201(5)	4090(6)	899(6)	212(33)
B2	1252(4)	3251(5)	4078(5)	74(35)
F12	1650(4)	3226(5)	3193(5)	130(20)
F22	1851(4)	3854(5)	5075(5)	120(19)
F32	549(4)	3599(5)	4013(5)	223(34)
F42	959(4)	2326(5)	4029(5)	175(26)
B3*	4222(10)	8627(11)	6602(10)	160(10)
F13*	3443(10)	7898(11)	6001(10)	244(61)
F23*	4591(10)	9017(11)	5911(10)	269(61)
F33*	4059(10)	9344(11)	7483(10)	181(43)
F43*	4795(10)	8249(11)	7012(10)	212(52)
B3' **	4308(19)	8767(24)	6724(24)	160(10)
F13' **	3842(19)	7902(24)	5823(24)	160(10)
F23' **	4388(19)	8615(24)	7689(24)	160(10)
F33' **	5133(19)	9110(24)	6549(24)	160(10)
F43' **	3868(19)	9440(24)	6833(24)	160(10)

^a Nonunity factors are starred: $\rightarrow = 0.666$, $** = 0.333$, $*** = 0.5$.

^b $U_{\text{eq}} = 1/3 \sum_i \sum_j U_{ij} a_i^* a_j^* a_i a_j$.

(23) Sugiyarto, K. H.; Goodwin, H. A. *Aust. J. Chem.* **1994**, *47*, 263.

(24) Vos, G.; de Graaff, R. A. G.; Haasnoot, J. G.; van der Kraan, A. M.; de Vaal, P.; Reedijk, J. *Inorg. Chem.* **1984**, *23*, 2905.

(25) Ainsworth, C.; Easton, N. R.; Livezey, M.; Morrison, D. E.; Gibson, W. R. *J. Med. Pharm. Chem.* **1962**, *5*, 383.

Table 4. Atomic Coordinates and Equivalent isotropic Thermal Factors for the Non-Hydrogen Atoms of [Fe₃(*p*-MeOtrz)₆(H₂O)₆](tos)₆·2CH₃OH·8H₂O (**2a**·2CH₃OH·8H₂O)^a

	X	Y	Z	U ^b		X	Y	Z	U ^b
Fe1	0	5000	5000	38(1)	S1	-7700(1)	4245(1)	2646(1)	65(2)
Fe2	-2764.0(0.5)	5599.3(0.4)	4361.2(0.4)	43(1)	O11	-6634(3)	4472(2)	3453(2)	68(5)
O1	4507(2)	5351(2)	6617(2)	59(4)	O21	-8508(3)	4621(3)	2844(3)	100(6)
O2	3526(3)	3846(2)	4808(2)	64(4)	O31	-7344(4)	4503(3)	2001(3)	95(6)
O3	2957(3)	3400(2)	6183(2)	70(5)	C11	-8459(4)	3020(4)	2167(3)	62(7)
N1a	-44(3)	3613(2)	4439(2)	46(5)	C21	-7867(5)	2481(5)	1977(4)	95(10)
N2a	960(3)	3416(2)	4637(2)	48(5)	C31	-8476(8)	1511(5)	1608(5)	122(13)
C3a	573(4)	2521(3)	4176(3)	52(6)	C41	-9684(9)	1086(5)	1421(5)	117(14)
N4a	-638(3)	2116(2)	3694(2)	43(4)	C51	-10233(7)	1633(6)	1610(5)	128(14)
C5a	-978(3)	2833(3)	3884(3)	46(6)	C61	-9652(6)	2585(5)	1979(4)	103(11)
C6a	-1387(4)	1157(3)	3113(3)	46(5)	C71	-10332(12)	-1(6)	1003(7)	195(22)
C7a	-2461(4)	927(3)	2390(3)	57(6)	S2	-1(1)	8028(1)	3930(1)	80(2)
C8a	-3176(4)	-12(3)	1835(3)	59(6)	O12	131(4)	7251(3)	4126(3)	139(9)
C9a	-2821(4)	-704(3)	1991(4)	68(7)	O22	-1157(3)	8036(3)	3848(3)	104(7)
C10a	-1765(5)	-458(3)	2714(4)	77(8)	O32	995(4)	8904(3)	4520(3)	104(7)
C11a	-1060(4)	465(3)	3286(3)	66(7)	C12	-84(5)	7808(4)	2857(4)	81(8)
O12a	-3589(4)	-1590(3)	1397(3)	104(7)	C22	-885(8)	6976(5)	2168(6)	129(14)
C13a	-3154(9)	-2304(5)	1501(8)	199(21)	C32	-1017(15)	6811(10)	1311(8)	200(29)
N1b	2092(3)	4960(2)	6567(2)	46(5)	C42	-332(14)	7467(13)	1124(8)	203(32)
N2b	1067(3)	5136(2)	6322(2)	45(4)	C52	492(10)	8282(10)	1812(8)	190(23)
C3b	930(4)	5413(3)	7050(3)	51(6)	C62	637(6)	8474(5)	2697(5)	120(12)
N4b	1810(3)	5425(3)	7754(2)	54(5)	C72	-399(15)	7360(13)	191(7)	352(44)
C5b	2512(4)	5148(3)	7415(3)	57(6)	S3	-4274(2)	2457(1)	2409(1)	107(3)
C6b	2015(5)	5730(4)	8671(4)	80(8)	O13*	-3327(4)	2661(3)	2166(4)	67(7)
C7b	1081(6)	5520(4)	8876(4)	104(11)	O23*	-3726(5)	2529(5)	3357(3)	93(9)
C8b	1388(7)	5815(4)	9852(5)	113(12)	O33*	-4994(5)	2950(4)	2288(6)	153(14)
c9b	2549(6)	6246(6)	10408(5)	110(12)	C13	-5247(5)	1269(4)	1772(4)	70(8)
C10b	3462(8)	6536(9)	10230(6)	171(20)	C23	-5587(6)	687(6)	2164(6)	104(11)
C11b	3168(7)	6194(7)	9336(4)	142(15)	C33	-6285(7)	-248(7)	1662(8)	144(17)
O12b	2879(5)	6616(5)	11363(3)	149(11)	C43	-6669(8)	-633(5)	799(7)	133(15)
C13b	2053(8)	6458(6)	11691(6)	153(16)	C53	-6325(8)	-53(5)	398(5)	128(14)
N1c	1610(3)	5623(2)	4851(2)	44(4)	C63	-5626(7)	894(4)	884(5)	102(11)
N2c	2627(3)	5433(2)	5095(2)	43(4)	C73	-7365(13)	-1698(9)	330(11)	275(33)
C3c	3419(3)	6010(3)	4958(3)	43(5)	OMe1	2825(4)	1940(3)	4280(3)	100(6)
N4c	2966(3)	6565(2)	4626(2)	44(4)	CMe1	3196(7)	1416(5)	3737(5)	137(13)
C5c	1831(3)	6291(3)	4575(3)	47(6)	OW1	8313(4)	9175(3)	5029(3)	115(7)
C6c	3534(4)	7284(3)	4397(3)	50(6)	OW2	4876(4)	6010(3)	2304(3)	126(8)
C7c	3245(5)	8055(3)	4520(4)	76(8)	OW3	5160(8)	4982(7)	861(6)	269(20)
C8c	3767(5)	8753(4)	4281(4)	89(9)	OW41*	3897(27)	3108(22)	774(19)	325(15)
C9c	4563(4)	8691(4)	3924(4)	74(8)	OW42**	3760(12)	3712(10)	935(9)	154(4)
C10c	4852(4)	7933(4)	3815(4)	76(8)	O43**	-4627	2908	2964	107
C11c	4308(4)	7216(3)	4035(3)	66(7)	O53**	-3155	2608	2931	107
O12c	5008(4)	9416(3)	3704(3)	114(7)	O63**	-4137	2958	1922	107
C13c	5924(7)	9429(7)	3431(6)	166(16)					

^a Nonunity factors are starred: * = 0.666, ** = 0.333. ^b U_{eq} = 1/3 Σ_i U_{ii} a_i² a_j² a_k².

follows: a solution of 379.3 mg (1.12 mmol) of iron(II) tetrafluoroborate hexahydrate in 5 mL of methanol was added to a solution of 498.3 mg (2.84 mmol) of *p*-MeOtrz in 5 mL of methanol. After a few minutes a colorless precipitate appeared. Single crystals suitable for X-ray structure determination were obtained by slow diffusion of diethyl ether in the mother liquid. The noncoordinated water molecules revealed by the X-ray structure are very easily removed, even at room temperature, so the chemical analysis yields a formula with only the four coordinated water molecules. Anal. Calcd for C₇₂H₈₀N₂₄O₁₂B₆F₂₄·Fe₃ (1): C, 40.00, H, 3.73; N, 15.55; B, 2.43; Fe, 7.75. Found: C, 40.81; H, 3.99, N, 15.75; B, 2.46, Fe, 7.51. The other trinuclear species, [Fe₃(*p*-MeOtrz)₆(H₂O)₆](tos)₆ (**2a**), was prepared as follows: a solution of 361.1 mg (0.71 mmol) of iron(II) tosylate hexahydrate in 1.5 mL of hot ethanol with one drop of water was added to a solution of 249.6 mg (1.42 mmol) of *p*-MeOtrz also in 1.5 mL of hot ethanol with one drop of water. On cooling a colorless precipitate appeared. Single crystals were obtained by slow diffusion of diethyl ether in a 90/10 methanol/water mixture. Some noncoordinated solvent molecules revealed by the X-ray structure are very easily removed at room temperature, and the chemical analysis yields a formula with only four noncoordinated water molecules. Anal. Calcd for C₉₆H₁₁₆N₁₈O₃₄S₆·Fe₃ (**2a**·4H₂O): C, 47.53; H, 4.82; N, 10.39; S, 7.93; Fe, 6.94. Found: C, 47.57; H, 4.91; N, 10.21; S, 7.64; Fe, 6.94. Heating a sample of **2a**·4H₂O at 100 °C for a short while afforded the compound **2b**, which is purple at room temperature, while **2a**·4H₂O is white at 290 °K, and turns purple on cooling. Anal. Calcd for C₉₆H₁₀₂N₁₈O₂₇S₆Fe₃ (**2b**):

C, 50.11; H, 4.46; N, 10.86; S, 8.60; Fe, 7.26. Found: C, 50.14; H, 4.47; N, 10.96; S, 8.36; Fe, 7.28.

Crystallographic Data Collection and Structure Determination.

Single crystals of compounds **1**·2H₂O (0.15 × 0.15 × 0.15 mm³) and **2**·2CH₃OH·8H₂O (0.15 × 0.25 × 0.50 mm³) were mounted on a Philips PW1100 diffractometer using graphite-monochromated Mo Kα radiation. The main crystallographic data are summarized in Tables 1 and 2. The data collections were performed with the following scanning conditions: ω/2θ mode, speed 0.03° s⁻¹ for **1** and 0.04° s⁻¹ for **2a**, width 1.5° for **1** and 1.2° for **2a**. From 5150 and 12 221 measured reflections, respectively, 2664 [level 2.5σ(I)] and 6938 [level 3σ(I)] were used. The structures were solved with the SHELXS86 program²⁶ and refined with the SHELXL76 program²⁷ to R-values of 0.084 and 0.056, respectively. Rigid blocks were used for phenyl and tetrafluoroborate groups. In **1** one of the BF₄⁻ groups along with a noncoordinated water molecule and in **2a** one of the tosylate groups and a water molecule were found to be disordered. The atomic coordinates are listed in Tables 3 and 4, and the bond lengths and bond angles involving iron atoms are listed in Tables 5 and 6.

Magnetic Properties. These were carried out with two apparatuses, namely a Faraday-type magnetometer equipped with a He continuous-

(26) Sheldrick, G. M. *SHELXS86, Program for Crystal Structure Solution*, University of Göttingen, Germany, 1986.

(27) Sheldrick, G. M. *SHELXL76, Program for Crystal Structure Determination*, University of Cambridge, U.K., 1976.

Table 5. Bond Lengths (Å) and Angles (deg) Involving the Iron Atoms in $[\text{Fe}_3(p\text{-MeOptrz})_8(\text{H}_2\text{O})_4](\text{BF}_4)_2 \cdot 2\text{H}_2\text{O}$ ($1 \cdot 2\text{H}_2\text{O}$)

Fe1–N1a	2.238(11)	N1a–Fe1–N1b	89.2(4)	Fe1–N1a–N2a	121.5(8)
Fe1–N1b	2.141(12)	N1a–Fe1–N1c	88.6(4)	Fe1–N1a–C5a	129.1(11)
Fe1–N1c	2.146(12)	N1b–Fe1–N1c	88.5(4)	Fe2–N2a–N1a	128.0(9)
Fe2–N2a	2.105(13)	N2a–Fe2–N2b	90.3(5)	Fe2–N2a–C3a	129.3(10)
Fe2–N2b	2.154(12)	N2a–Fe2–N2d	97.0(5)	Fe1–N1b–N2b	125.6(9)
Fe2–N2d	2.180(15)	N2a–Fe2–OW1	89.2(4)	Fe1–N1b–C5b	130.5(10)
Fe2–OW1	2.159(9)	N2a–Fe2–OW2	176.6(4)	Fe2–N2b–N1b	123.8(9)
Fe2–OW2	2.153(12)	N2b–Fe2–N2d	94.0(5)	Fe2–N2b–C3b	129.0(11)
Fe2'–N2c	2.167(13)	N2b–Fe2–OW1	176.3(5)	Fe1–N1c–N2c	123.9(9)
		N2b–Fe2–OW2	91.7(5)	Fe1–N1c–C5c	131.8(10)
		N2d–Fe2–OW1	89.7(5)	Fe2'–N2c–N1c	125.5(9)
		N2d–Fe2–OW2	85.6(5)	Fe2'–N2c–C3c	126.2(11)
		OW1–Fe2–OW2	88.6(4)	Fe2–N2d–N1d	113.7(11)
				Fe2–N2d–C3d	135.5(12)

Table 6. Bond Lengths (Å) and Angles (deg) Involving the Iron Atoms in $[\text{Fe}_3(p\text{-MeOptrz})_6(\text{H}_2\text{O})_6](\text{tos})_7 \cdot 2\text{CH}_3\text{OH} \cdot 8\text{H}_2\text{O}$ ($2a \cdot 2\text{CH}_3\text{OH} \cdot 8\text{H}_2\text{O}$)

Fe1–N1a	2.192(4)	N1a–Fe1–N2b	89.8(1)	Fe1–N1a–N2a	124.5(3)
Fe1–N2b	2.164(3)	N1a–Fe1–N1c	90.0(1)	Fe1–N1a–C5a	128.0(3)
Fe1–N1c	2.174(4)	N2b–Fe1–N1c	91.1(1)	Fe2'–N2a–N1a	121.3(3)
Fe2'–O1	2.077(3)	O1–Fe2'–O2	88.3(1)	Fe2'–N2a–C3a	132.1(3)
Fe2'–O2	2.224(4)	O1–Fe2'–O3	85.5(1)	Fe2'–N1b–N2b	122.4(3)
Fe2'–O3	2.275(4)	O1–Fe2'–N2a	171.3(1)	Fe2'–N1b–C5b	130.2(3)
Fe2'–N2a	2.215(4)	O1–Fe2'–N1b	89.7(1)	Fe1–N2b–N1b	124.9(3)
Fe2'–N1b	2.145(4)	O1–Fe2'–N2c	94.8(1)	Fe1–N2b–C3b	129.1(3)
Fe2'–N2c	2.012(4)	O2–Fe2'–O3	81.0(1)	Fe1–N1c–N2c	126.7(3)
		O2–Fe2'–N2a	88.2(1)	Fe1–N1c–C5c	125.6(3)
		O2–Fe2'–N1b	169.1(1)	Fe2'–N2c–N1c	122.7(3)
		O2–Fe2'–N2c	95.1(1)	Fe2'–N2c–C3c	130.4(3)
		O3–Fe2'–N2a	86.1(1)		
		O3–Fe2'–N1b	88.2(1)		
		O3–Fe2'–N2c	176.1(1)		
		N2a–Fe2'–N1b	92.2(1)		
		N2a–Fe2'–N2c	93.4(1)		
		N1b–Fe2'–N2c	95.8(1)		

flow cryostat working in the 4.2–450 K temperature range, and a SQUID magnetometer working down to 1.7 K. The data were corrected of the diamagnetism of the core estimated from Pascal's tables.

Mössbauer Spectra. These were obtained on a constant-acceleration spectrometer with a 25 mCi source of ^{57}Co in a rhodium matrix. The calibration was made with a metallic iron foil at room temperature. The absorbers were samples of about 120 mg of compound **1** or **2a** spread over 3 cm² area in a home-designed sample holder maintained in a primary vacuum. The typical counting time was ca. 6 h. A least-squares computer program was used to fit the Mössbauer parameters and to determine their standard deviations of statistical origin.

Description of the Structures

The structures of both **1** and **2a** consist of linear trinuclear cations with +6 charges shown in Figures 1 and 2, and noncoordinated monovalent anions and solvent molecules. For both compounds the central iron atom is located on an inversion center and is surrounded by six *p*-MeOptrz ligands. The FeN_6 core involving the central atom is an almost perfect octahedron; the bond angles are all very close to either 90° or 180°. The Fe–N bond lengths at room temperature (average value equal to 2.175 Å) are typical of iron(II) high-spin compounds. This central atom is bridged to each of the two external iron atoms by three *p*-MeOptrz ligands through the nitrogen atoms in the 1,2-positions.

For **1**, each external iron atom is surrounded by three bridging and one terminal *p*-MeOptrz ligands, the octahedral environment being completed by two water molecules. We will see below that the dihedral angles between the triazole and phenyl rings of the *p*-MeOptrz ligands are important structural parameters. For the bridging ligands occupying *trans* positions with respect to the terminal water molecules (noted a and b in Figure 1) these dihedral angles are equal to 80.8 and 88.0°. For the third bridging ligand (noted c in Figure 1) the value of this angle is 45.3°. Finally, for the terminal *p*-MeOptrz ligand, the dihedral angle is equal to 17.4°.

The X-ray analysis sees two noncoordinated water molecules which are hydrogen bonded to the coordinated water molecules. These noncoordinated water molecules are very easily removed from the lattice.

For **2a** the environment of the central iron atom is very similar to that found for **1**. On the other hand, each external iron atom is surrounded by three *p*-MeOptrz bridging ligands and three water molecules. The values of the dihedral angles between triazole and phenyl rings of the ligands are 33.3°, 36.3°, and 29.9°.

The X-ray analysis also reveals two methanol and eight water molecules hydrogen bonded to the trinuclear units. Some of these noncoordinated molecules may be removed from the lattice at room temperature.

Magnetic Properties

Compound 1. The magnetic behavior of **1** is shown in Figure 3 in the form of the $\chi_M T$ versus T plot, χ_M being the molar magnetic susceptibility and T the temperature. At 335 K, $\chi_M T$ is equal to 9.33 cm³ K mol^{−1}, which corresponds to what is expected for three noninteracting high-spin iron(II) ions. As T is lowered, $\chi_M T$ decreases more and more rapidly and reaches 1.1 cm³ K mol^{−1} at 1.7 K. This behavior is due to the combined effect of intramolecular antiferromagnetic interactions and local anisotropies. To interpret quantitatively these data, we considered the zero-field spin Hamiltonian

$$\mathbf{H} = -J\mathbf{S}_B \cdot (\mathbf{S}_A + \mathbf{S}_C) + D_A(\mathbf{S}_{A,z}^2 + \mathbf{S}_{C,z}^2) + D_B\mathbf{S}_{B,z}^2 \quad (1)$$

and the Zeeman perturbation

$$\mathbf{H}_{ZE} = g\beta(\mathbf{S}_A + \mathbf{S}_B + \mathbf{S}_C) \cdot \mathbf{H} \quad (2)$$

The first term in the right-hand side of eq 1 describes the isotropic interaction between the central iron(II) ion noted B

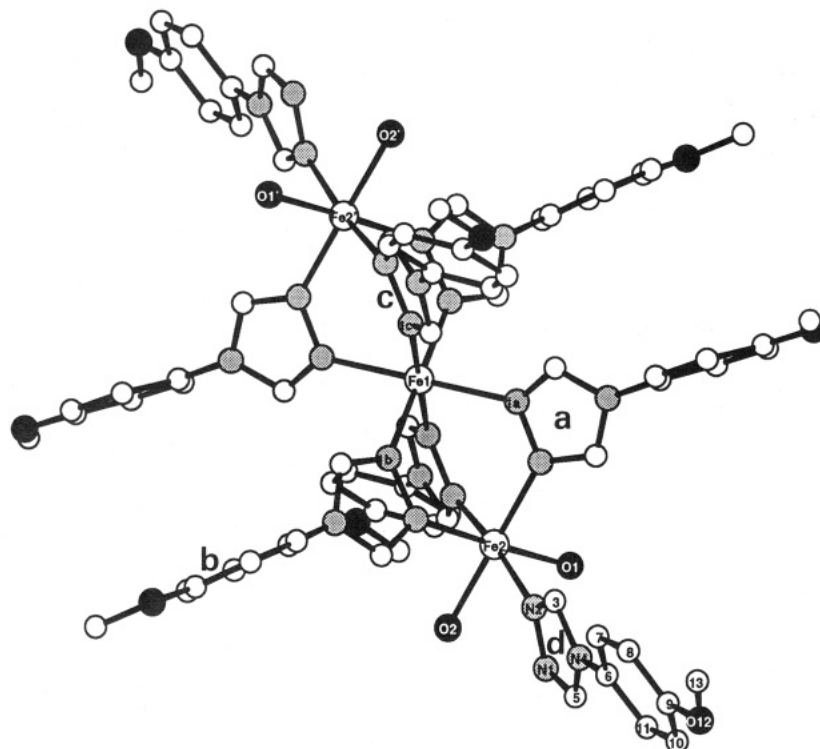


Figure 1. View of the $[\text{Fe}_3(\text{p-MeOptrz})_8(\text{H}_2\text{O})_4]^{6+}$ trinuclear cation in compound **1**·2H₂O. H-atoms were omitted for clarity. Oxygen atoms are black, and nitrogen atoms are shaded.

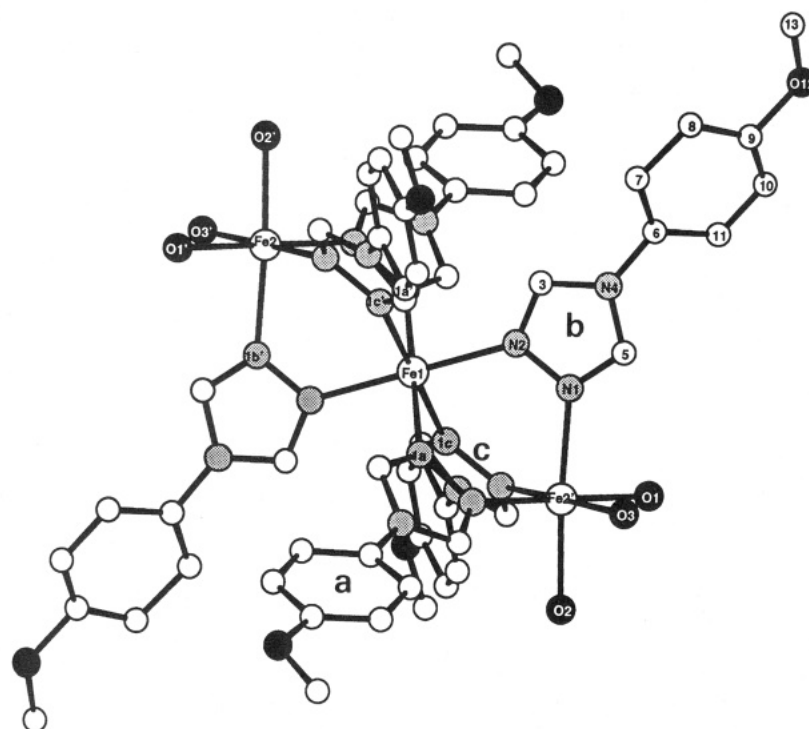


Figure 2. View of the $[\text{Fe}_3(\text{p-MeOptrz})_6(\text{H}_2\text{O})_6]^{6+}$ trinuclear cation in compound **2a**·2CH₃OH·8H₂O. H-atoms were omitted for clarity. Oxygen atoms are black, and nitrogen atoms are shaded.

and the two external iron(II) ions noted A and C, J being the isotropic interaction parameter. The second and third terms describe the local anisotropies of the metal ions, D_A and D_B being the axial zero-field splitting parameters for the external and central ions, respectively. For the three ions, the local anisotropy is assumed to be axial, the axis being the internuclear direction. In (1) the anisotropic interaction parameter is assumed to be negligible. In the Zeeman perturbation (2) the local g -tensors are assumed to be isotropic with the same principal value, g . The zero-field energies, $E_n(0)$, and eigenvectors,

$[\Psi_n(0)]$, were determined by full diagonalization of (1) using the 125 $|S, S', M_S\rangle$ kets as a basis set. S and S' are the quantum numbers associated with the spin operators S and S' , respectively, with

$$S' = S_A + S_C \quad (3)$$

$$S = S' + S_B \quad (4)$$

The first- and second-order Zeeman coefficients for both the

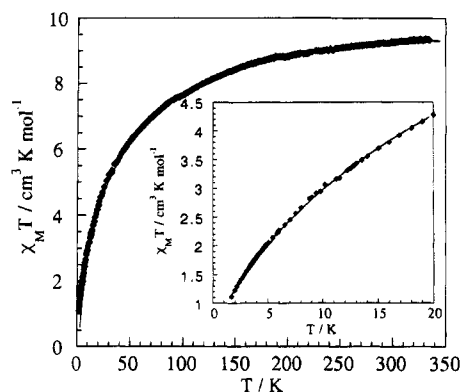


Figure 3. Experimental (♦) and calculated (—) $\chi_M T$ versus T plot for compound **1**. The insert emphasizes the low-temperature data.

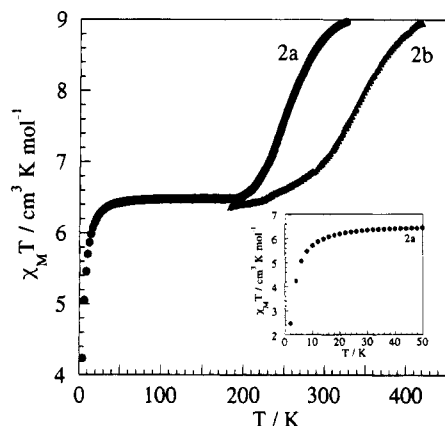


Figure 4. $\chi_M T$ versus T plots for compounds **2a**·4H₂O and **2b**. The insert emphasizes the data below 50 K for **2a**.

parallel and perpendicular directions of the applied magnetic field H were calculated by diagonalizing $\mathbf{H} + \mathbf{H}_{ZE}$, using the $[\Psi_n(0)]$ functions as a new basis set. The average susceptibility χ_M was approximated by $(\chi_z + 2\chi_x)/3$, where χ_z and χ_x are the principal susceptibilities. Such an approximation is known to be valid when the applied field is low. In order to avoid an overparametrization of the problem, we did not try to determine separately the D_A and D_B parameters. Instead, we solved the problem assuming that D_B was negligible as compared to D_A . This assumption is justified by the fact that the FeN₆ core involving the central ion is an almost perfect octahedron. The minimization of the agreement factor R defined by $\sum[(\chi_M T)^{\text{obs}} - (\chi_M T)^{\text{cal}}]^2 / \sum[(\chi_M T)^{\text{obs}}]^2$ led to $J = -5.70 \text{ cm}^{-1}$, $D_A = 7.21 \text{ cm}^{-1}$, and $g = 2.10$. R is then equal to 3.3×10^{-4} , which corresponds to an excellent theory–experiment agreement (see Figure 3). In particular, the sign of D_A is known unambiguously. As a matter of fact, the antiferromagnetic interaction between central and external iron(II) ions lead to a ground spin state defined by $S = 2$, $S' = 4$. This spin state is split in zero field by D_A to give an $M_s = 0$ ground state, if D_A is positive, or an $M_s = \pm 2$ ground state, if D_A is negative. In the former case the low-temperature limit of $\chi_M T$ is zero; in the latter case, it is $Ng^2\beta^2/3k$ (ca. $2.21 \text{ cm}^3 \text{ K mol}^{-1}$). The curve of Figure 3 clearly shows that $\chi_M T$ decreases much below $2.21 \text{ cm}^3 \text{ K mol}^{-1}$ as T is lowered below ca. 4.8 K and tends to zero when T approaches absolute zero.

The assumption that D_B is negligible as compared to D_A might be questionable. Indeed, as we will see below, the central and terminal iron sites are not distinguishable in Mössbauer spectroscopy. That is why we also fitted the magnetic data in assuming that D_A and D_B are equal, which led to $D_A = D_B = 5.75 \text{ cm}^{-1}$ with the same values of g and J . The agreement

Table 7. Isomer Shift (IS), Half-Height Width (Γ), and Quadrupole Splitting (QS) for $[\text{Fe}_3(p\text{-MeOtr})_8(\text{H}_2\text{O})_4](\text{BF}_4)_2$ (**1**) at Some Selected Temperatures^a

T (K)	IS (mm s ⁻¹)	Γ (mm s ⁻¹)	QS (mm s ⁻¹)
4.2	1.206(1)	0.384(3)	3.292(2)
78	1.197(1)	0.382(2)	3.316(2)
292	1.083(2)	0.330(7)	2.810(5)

^a Mean-squares deviations of statistical origin are given in parentheses. Isomer shifts are referred to metallic iron at room temperature.

factor R is then equal to 4.7×10^{-4} , which is a little bit higher than in the former hypothesis.

Compounds 2a·4H₂O and 2b. $\chi_M T$ for **2a**·4H₂O is equal to $9.0 \text{ cm}^3 \text{ K mol}^{-1}$ at 330 K, decreases as T is lowered down to ca. 200 K, and then reaches a plateau in the 200–60 K temperature range with $\chi_M T = 6.5 \text{ cm}^3 \text{ K mol}^{-1}$. As T is lowered further below ca. 60 K, $\chi_M T$ decreases again more and more rapidly and reaches $2.5 \text{ cm}^3 \text{ K mol}^{-1}$ at 1.8 K. Between 330 and 200 K, $\chi_M T$ loses one-third of its value, which corresponds to a gradual $S = 2 \leftrightarrow S = 0$ spin conversion for the central iron(II) ion of the trinuclear unit, the two external ions remaining in the high-spin state. This behavior does not show any thermal hysteresis. The temperature for which the low-spin and high-spin molar fractions for the central ion(II) are both equal to 0.5, $T_{1/2}$, is found as 245 K. The magnetic data below ca. 60 K may be attributed to both the local anisotropy of the terminal high-spin iron(II) ions and a very weak antiferromagnetic interaction between these ions through the central low-spin ion. We did not try to fit the data with a model taking into account the two phenomena; the axial zero-field splitting parameter D and interaction parameter J are too correlated. Rather, we assumed that the local anisotropy which is known to be important for high-spin iron(II) ions was the dominant phenomenon. In this frame, the data are fairly well fitted with $D = 7.1 \text{ cm}^{-1}$. We may notice that this value is very close to that determined for the external Fe(II) ions of compound **1**.

2b shows a rather similar behavior with a spin transition for one of the three iron(II) ions. This transition, however, is a bit smoother and is displaced toward high temperatures. $T_{1/2}$ is found as 330 K.

Mössbauer Data

Compound 1. The Mössbauer spectra of compound **1** are characteristic of high-spin iron(II) ions at any temperature. They do not distinguish the central and terminal metal sites. The spectra also show a small amount of a low-spin impurity, the proportion of which does not vary versus temperature. Least-squares fitted parameters at selected temperatures are reported in Table 7.

Compound 2a·4H₂O. The spectra of compound **2a**·4H₂O distinguish the two high-spin sites above ca. 280 K and reveal the spin transition for the central iron(II) ion as T is lowered. Some typical spectra are shown in Figure 5. Least-squares fitted parameters are listed in Table 8. At 310 K the spectrum is essentially that of two high-spin sites in the 2/1 ratio. The spin transition begins around room temperature and is complete at ca. 190 K, which is perfectly in line with the magnetic susceptibility data. The temperature dependence of the high-spin molar fraction for the central iron(II) ion as deduced from the Mössbauer data is represented in Figure 6.

Discussion

We will first discuss the crystal structures of compounds **1** and **2a** and then the magnetic properties and spin transition behaviors.

Table 8. Isomer Shift (IS), Half-Height Width (Γ), and Quadrupole Splitting (QS) Relative Area, and Spin State for [Fe₃(*p*-MeOtrz)₆(H₂O)₆](tos)₆·4H₂O (**2a**·4H₂O) at Some Selected Temperatures^a

<i>T</i> (K)	IS (mm s ⁻¹)	Γ (mm s ⁻¹)	QS (mm s ⁻¹)	relative area (%)	spin state
4.2	1.246(1)	0.284(3)	3.428(2)	67	HS
	0.566(2)	0.236(5)	0.14(1)	33	LS
77	1.232(1)	0.262(3)	3.421(2)	67	HS
	0.546(2)	0.256(7)	0.13(1)	33	LS
120	1.223(1)	0.266(4)	3.393(3)	67	HS
	0.555(2)	0.252(9)	0.12(1)	33	LS
160	1.206(1)	0.276(3)	3.337(2)	66	HS
	0.547(2)	0.254(7)	0.12(1)	34	LS
180	1.198(1)	0.276(2)	3.318(1)	66	HS
	0.547(1)	0.252(4)	0.12(1)	34	LS
210	1.180(1)	0.304(2)	3.244(2)	73	HS
	0.537(2)	0.282(8)	0.11(1)	27	LS
220	1.171(1)	0.328(4)	3.186(2)	79	HS
	0.526(5)	0.40(1)	0.11	21	LS
240	1.127(5)	0.33	2.86(2)	66.7	HS _c
	1.168(1)	0.296(3)	3.183(5)	21.5	HS _c
	0.529	0.400	0.10	11.8	LS
260	1.166(2)	0.306(6)	3.107(4)	66.7	HS _c
	1.080(8)	0.50	2.73(2)	29.6	HS _c
	0.529	0.400	0.10	3.6	LS
280	1.167(2)	0.328(6)	3.045(4)	66	HS _c
	0.97(1)	0.328(6)	2.80(2)	27	HS _c
	0.52	0.66	0.12	6	LS
292	1.137(3)	0.306(5)	2.959(6)	66	HS _c
	0.983(6)	0.306(5)	2.54(1)	31	HS _c
	0.52	0.66	0.12	2	LS

^a mean-squares deviations of statistical origin are given in parentheses. Isomer shifts are referred to metallic iron at room temperature. HS refers to the high-spin state for the two iron sites; HS_c and HS_e refer to the high-spin state for the external and central iron sites, respectively. LS refers to the low-spin state. The italic values were fixed during the fitting.

Trinuclear structures relevant to the structure of compound **1** with six bridging and two terminal triazole ligands were already reported with Co(II) and Ni(II) ions; the additional terminal positions are then occupied by NCS anions.^{28,29} One iron(II) compound containing both terminal and bridging triazole ligands has been reported. This compound, of formula Fe₂(ptrz)₅(NCS)₄ with ptrz = 4-propyl-1,2,4-triazole, has a binuclear structure with three bridging and two terminal ptrz ligands.³⁰

As already mentioned, a structure similar to that of compound **2a** has already been described by Reedijk and co-workers, the bridging ligands being 4-ethyl-1,2,4-triazole.²⁴ The FeN₆ cores involving the central iron atoms in their high-spin state are much the same in **2a** and Reedijk's compound. It is also worthwhile to compare the FeN₆ core in **2a** with the environment of the iron(II) ion in bis[hydrotris(1-pyrazolyl)borato]iron(II) and bis[hydrotris(3,5-dimethylpyrazolyl)borato]iron(II).^{31,32} The former compound is low-spin at room temperature, and exhibits a low-spin → high-spin transition upon heating. The average value of the Fe–N bond lengths at room temperature, 1.973(7) Å, is much shorter than in **2a** at the same temperature. The latter compound is high-spin in the whole temperature range; the average value of the Fe–N bond lengths, 2.172(2) Å, is much the same as in **2a**.

Concerning the structures of Fe(II)–1,2,4-triazole compounds, a point deserves to be discussed briefly, namely the duality

between trinuclear and polymeric structures. The tendency for 4-substituted-1,2,4-triazole ligands to afford trinuclear species seems to be more pronounced as the substituent on the 4-position becomes bulkier. For instance, 4-amino-1,2,4-triazole gives polymeric structures while 4-(dimethylamino)-1,2,4-triazole gives trinuclear units.

The main question raised by our findings concerns the spin state of the iron(II) ions. In **1** the three metal ions are high-spin in the whole temperature range. This allowed us to determine accurately for the first time the interaction parameter between two iron(II) ions triply bridged by triazole ligands. In contrast, the central iron(II) ion in **2a** undergoes a gradual spin conversion centered around 245 K. This difference, at the first view, is surprising since the two FeN₆ cores in **1** and **2a** are very similar at room temperature, with average values of the Fe–N bond lengths equal to 2.175 and 2.177 Å, respectively. The Fe–Fe separations between central and external metal ions are also very close to each other, 3.868(2) Å in **1** and 3.8789(6) Å in **2a**. The principal difference between the two structures, in addition to the presence of terminal triazole ligands in **1**, concerns the dihedral angles between the triazole and phenyl rings of the bridging *p*-MeOptrz ligands. The average value of this angle is 71.4° in **1**, and 33.2° in **2a**. It follows that the conjugation between the two rings is significantly more pronounced in this latter case. The methoxy group on the phenyl ring in the *trans*-position is expected to exert an electron-donating effect which may be transmitted to the coordinating nitrogen atoms through the conjugation between the two rings. This effect is transmitted more efficiently in **2a** than in **1**. In other words the ligand field exerted on the central iron(II) ion may be anticipated to be stronger in **2a**. The variation of the dihedral angle creates a sort of switching effect between the high-spin and spin-conversion situations. A further decrease of the angle is anticipated to stabilize the low-spin phase, i.e. to shift the inversion temperature *T*_{1/2} toward the higher temperatures. Of course in the present case we do not control this switching. The fact that the *p*-MeOptrz ligands are more coplanar in **2a** might be due to the shape of the anions. The little and rather spherical tetrafluoroborate anion fits the space between the phenyl rings while the aromatic ring of the tosylate anion forces the rings of *p*-MeOptrz to be coplanar.

The dehydration of **2a** affords **2b**, the structure of which is unknown. The chemical analysis reveals that **2b** contains only one water molecule per iron atom, which is not sufficient for isolated [Fe₃(*p*-MeOptrz)₆(H₂O)₆]⁶⁺ trinuclear units. However, the infrared spectrum of **2b** does not differ much from that of **2a**, the main difference being the decrease in intensity of the band around 3400 cm⁻¹ due to noncoordinated water. Perhaps some water molecules in **2b** bridge the trinuclear units. In any case the spin conversion again concerns only one out of three iron(II) ions; it is even more gradual than in **2a**·4H₂O, and *T*_{1/2} is displaced toward higher temperatures by about 85 K. The fact that the dehydration makes the spin conversion more gradual is well-documented^{33,34} and is attributed to a decrease of the cooperativity propagated through the hydrogen bonds.³⁵ As for the influence of the dehydration on *T*_{1/2}, there is no general rule. For some compounds, removing noncoordinated water molecules results in a lowering of *T*_{1/2}. This effect may be so pronounced that the compound may become high-spin in the whole temperature range. Such a situation happens for *trans*-

(28) Groeneveld, L. R.; le Fèvre, R. A.; de Graaff, R. A. G.; Haasnoot, J. G.; Vos, G.; Reedijk, J. *Inorg. Chim. Acta* **1985**, *102*, 69.

(29) Haasnoot, J. G. *Comments Inorg. Chem.*, in press.

(30) Haasnoot, J. G., private communication.

(31) Hutchinson, B. B.; Daniels, L.; Henderson, E.; Neill, P. *J. Chem. Soc., Chem. Commun.* **1979**, 1003.

(32) Oliver, J. D.; Mullica, D. F.; Hutchinson, B. B.; Milligan, W. O. *Inorg. Chem.* **1980**, *19*, 165.

(33) Tweedle, M. F.; Wilson, M. *J. Am. Chem. Soc.* **1976**, *98*, 4824.

(34) Summerton, A. P.; Diamantis, A. A.; Snow, M. R. *Inorg. Chim. Acta* **1978**, *27*, 123.

(35) Claude, R.; Zarembowitch, J.; Philoche-Levisalles, M.; d'Yvoire, F. *New J. Chem.* **1991**, *15*, 635, and references therein.

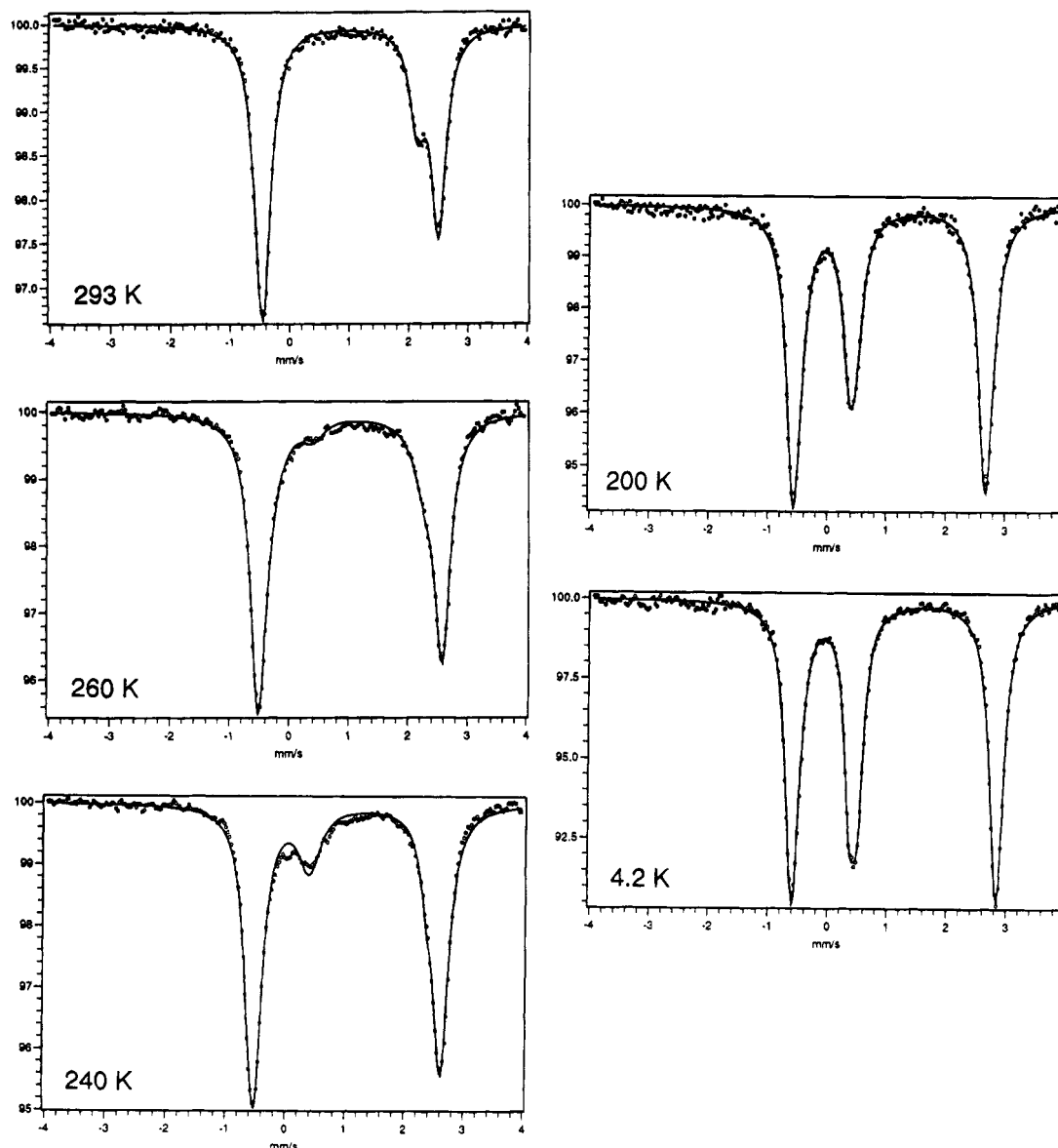


Figure 5. Mössbauer spectra of compound **2a**·4H₂O at various temperatures.

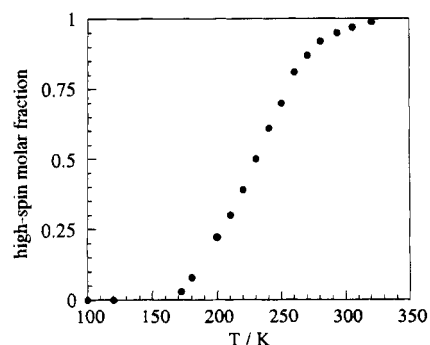


Figure 6. High-spin molar fraction versus temperature for the central iron(II) ion of compound **2a**·4H₂O as deduced from the Mössbauer spectra.

bis(thiocyanato)bis(4,4'-bis-1,2,4-triazole)iron(II) monohydrate.³⁶ In other compounds, a rising of $T_{1/2}$ is observed upon dehydration. That is what happens between **2a**·4H₂O and **2b**. Perhaps, in that case, the dehydration increases further the coplanarity of the *p*-MeOptrz ligands. A similar shift of $T_{1/2}$ has been found

for bis[2,6-bis(triazol-3-yl)pyridine]iron(II) chloride.³⁷ This compound, which crystallizes with three water molecules, undergoes a partial spin conversion at low temperature. Removing the water molecules affords a new compound which is low-spin at room temperature.

Concluding Remarks

A variation of the dihedral angle within the *p*-MeOptrz ligands seems to lead to a switching between high-spin and spin-conversion situations. There is another structural difference between **1** and **2a**, namely the presence of terminal *p*-MeOptrz ligands in **1**. This factor, however, does not seem to be crucial as far as this type of high-spin–spin-conversion switching is concerned. As a matter of fact, we also prepared the two compounds [Fe₃(*m*-Meptz)₆(H₂O)₆](BF₄)₆ and [Fe₃(*m*-Meptz)₆(H₂O)₆](tos)₆, with *m*-Meptz = 4-(*m*-methylphenyl)-1,2,4-triazole. In both the fluoroborate and tosylate derivatives the Fe/*m*-Meptz stoichiometry is equal to 1/2, which strongly suggests that all the *m*-Meptz ligands are bridging. The former compound behaves like **1**; the Fe(II) ions are high-spin in the

(36) Vreugdenhil, W.; van Diemen, J. H.; de Graaff, R. A. G.; Haasnoot, J. G.; Reedijk, J.; van der Kraan, A. M.; Kahn, O.; Zarembowitch, J. *Polyhedron* **1990**, *9*, 2971.

(37) Sugiyarto, K. H.; Craig, D. C.; Rae, A. D.; Goodwin, H. A. *Aust. J. Chem.* **1993**, *46*, 1269.

whole temperature range. The latter compound behaves like **2a**; the central ion undergoes a gradual spin conversion with $T_{1/2} = 200$ K. The fine tuning of the ST occurrence is certainly one of the important issues in the field of ST compounds. In the present case it would not be fair speaking of tuning. Indeed, the values of the phenyl–triazole dihedral angles are imposed by the nature of the anion. However, our findings suggest us that it would be worth exploring the chemical means to control the relative orientations of the two rings in *p*-MeOptrz and other similar 4-phenyl-substituted-1,2,4-triazole ligands.

In other respects, this work allowed us to determine the magnitude of the interaction parameter between two high-spin Fe(II) ions triply bridged by triazole ligands through the 1,2-positions. In polymeric species like [Fe(Htrz)(trz)](BF₄) or [Fe-

(Htrz)₃](BF₄)₂·H₂O the ST has a very strong cooperative character.³⁸ The question which we are faced with concerns the influence of the Fe(II)–Fe(II) interaction through the triazole ligands on the cooperativity.

Supplementary Material Available: Tables SI–SVIII listing the detailed crystallographic data, atomic coordinates, and isotropic temperature factors of the hydrogen atoms, anisotropic temperature coefficients of non-hydrogen atoms, and bond lengths and angles for compounds **1**·2H₂O and **2a**·2CH₃OH·8H₂O (11 pages). Ordering information is given on any current masthead page.

-
- (38) Kröber, J.; Audière, J. P.; Claude, R.; Codjovi, E.; Kahn, O.; Haasnoot, J. G.; Grolière, F.; Jay, C.; Boussekou, A.; Linarès, J.; Varret, F.; Gonthier-Vassal, A. *Chem. Mater.* **1994**, *6*, 1404.